International Journal of Applied Pharmaceutics

ISSN- 0975-7058 Vol 17, Issue 6, 2025

Original Article

ANTI-CANCER POSSIBILITY OF *ZINGIER OFFICIALE* NANOPARTICLES: MECHANISMS AND THERAPEUTIC UNDERSTANDING

NAJAT AMEEN SAEED, ABEER MANSOUR ABDEL RASOOL*, AYMN YASEEN SHARAF ZEEBAREE

Pharmacology and Toxicology Department, College of Pharmacy, Ninevah University-Ninevah City-Iraq
***Corresponding author: Abeer Mansour Abdel Rasool; *Email: abeer.mansour@uoninevah.edu.iq**

Received: 30 Jun 2025, Revised and Accepted: 15 Sep 2025

ABSTRACT

Objective: To synthesize and profile green-prepared copper nanoparticles (ZOE-CuNPs) and to determine their cytotoxicity effects on human breast cancer cells.

Methods: ZOE-CuNPs were synthesized by green reduction of copper acetate using *Zingiber officinale* extract. The characterization was done by UV-Vis, XRD, SEM-EDS, and FT-IR techniques. Cytotoxicity was assessed in aline of breast cancer cells. A new breast cancer cell line (AMJ13) using the MTT assay (3-[4,5-dimethylthiazol-2-yl]-2,5 diphenyltetrazolium bromide) at 0-100 µM concentrations.

Results: Copper nanoparticles were successfully synthesized using Zingiber officinale extract (ZOE-CuNPs) via green synthesis, as established by UV-Vis spectroscopy displayed distinguishing absorption peak at ~439 nm, characteristic of Cu-based nanoparticles; the spectra were unchanged after ageing. XRD noted Cu-based nanocrystalline phases (probably including copper oxides, e. g., Cu 2 O/CuO); a clear assignment would require application of Rietveld alteration against appropriate JCPDS cards with a regular particle dimension of 31 nm, calculated using means of the Debye-Scherrer equation. Scanning electron microscopy demonstrated predominantly quasi-spherical morphology with slight accumulation, although energy-dispersive X-ray spectroscopy confirmed elemental composition (Cu, O, C). FTIR analysis identified spectral shifts in the ranges 3248-3355 cm^{-1}, 1652-1751 cm^{-1}, and 1479-1432 cm^{-1}, indicating gingerol-mediated reduction and stabilization of copper ions through alcohol, carbonyl, and amine functional groups. Cytotoxicity evaluation against breast cancer cells using MTT assay revealed concentration-dependent anticancer activity across six concentrations (0-100 µM), with inhibition rates increasing from 0.00±2.1% (control) to 75.00±2.9% at 100 µM. Analysis(one-way ANOVA, $p<0.001$) confirmed significant differences between all concentration groups, demonstrating potent dose-dependent cytotoxic efficacy of the green-synthesized ZOE-CuNPs for potential anticancer nanomedicine applications.

Conclusion: ZOE-CuNPs exhibit high, concentration-dependent anticancer activities, which are likely mediated through ROS generation and initiation of apoptotic pathways.

Keywords: Breast cancer, Cytotoxicity, MTT assay, *Zingiber* officinale

DOI: https://dx.doi.org/10.22159/ijap.2025v17i6.55836 Journal homepage: https://innovareacademics.in/journals/index.php/ijap

INTRODUCTION

One of the important causes of death worldwide, cancer, is still a health concern with rising incidence rates and evolving resistance to conventional therapies. Traditional chemotherapeutic drugs tend to be hampered by low selectivity, systemic toxicity, low bioavailability, and the induction of multidrug resistance. These limitations drive the search for new, targeted, and biocompatible therapies that can potently inhibit tumor growth without producing adverse effects on normal tissues [1].

Parallel to this, the trend towards ecologically friendly means of nanomaterial synthesis has witnessed the emergence of green nanotechnology. Instead of using hazardous chemicals and energy-intensive procedures that are common in the manufacture of conventional nanoparticles, this technique uses biological resources, such as plant extracts, to act as reducing and stabilizing agents. One such precious bioresource is *Zingiber officinale* (ginger), a medicinal herb widely utilized in conventional medicine for its pharmacological versatility [2, 3].

The antioxidant, anti-inflammatory, antibacterial, and anticancer properties of ginger are attributed to its abundance of bioactive phytoconstituents, such as gingerol, shogaol, paradol, and zingerone. It has been suggested that the phytoconstituents alter many molecular targets implicated in carcinogenesis, including Nuclear Factor Kappa (NF-Kb). Nuclear factor erythroid 2-related factor (2Nrf2) and phosphoinositide 3-kinase/protein kinase B/mammalian target of rapamycin (PI3K/Akt/mTOR) also cause apoptosis in a number of cancer cell lines. Interestingly, the occurrence of functional groups within these compounds-hydroxyl, carbonyl, and amine functionalities—is the reason why they can serve the function of natural reducing and capping agents during metal nanoparticles biosynthesis, promoting their dispersion, stability, and bioactivity [3, 4].

Nanotechnological application of *Zingiber officinale* has emerged as an advanced frontier area of cancer therapy. Plant-mediated metal-based nanoparticle synthesis, such as zinc oxide, silver, and copper provides biocompatibility along with enhanced cellular uptake. Remarkably, zinc oxide nanoparticles (ZnONPs) and silver nanoparticles (AgNPs) of ginger have exhibited promising results in generating reactive oxygen speciesthat triggerapoptosis in cancer cells but leave normal cells unaffected. These findings qualify the employment of ginger extracts during the synthesis of nanoparticles as a means of achieving selective and effective targeting of cancer cells [5].

Under such a context, the present research focuses on copper nanoparticle green synthesis using Zingiber officinale extract (ZOE-CuNPs) and explores their anticancer potential and physicochemical properties. By merging the medicinal efficacy of ginger with the therapeutic properties of copper nanoparticles, this study intends to develop a biocompatible nanoplatform with enhanced anticancer efficacy. The produced ZOE-CuNPs were characterized by means of advanced analytical methods such as FT-IR, XRD, SEM, EDS, and UV-Vis spectroscopy. In order to ascertain their capacity to impede cell growth and induce apoptosis, their cytotoxicity was also evaluated using in vitro assays versus human cancer cell lines, namely breast cancer [6].

MATERIALS AND METHODS

Utilized materials

The salt of copper (II) acetate [purity: 98%; CAS No: 142-71-2; M. wt: 181.63 g/mol] that was used in this work was purchased from Sigma-Aldrich Company. The fresh rhizomes of *Zingiber officinale*

Voucher Specimen Number (ZO-MOS-2024-001) used in this study were obtained in the local herbal market of Mosul City, Nineveh governorate, Iraq (Geographical coordinates: 36.356601 N and 43.157501 E) in February 2024. The human breast cancer cells (AMJ13) were obtained IRAQ Biotech Cell Bank, Baghdad city, Iraq.

Preparation of 0.1M copper acetate solution [Cu $(CH_3CO_2)_2$]

For designing copper nanoparticles, a solution of 0.1M copper acetate was made in a conical flask [100 ml volume] with 1.8 g dissolved into 100 ml of distilled water. After that, the obtained precursor solution was stored in dark place until use.

Preparation of *Zingiber officinale* extracts (ZOE)

After washing and cleaning of *zingiber officinale pieces* and drying them in the sunlight, the dried pieces were crushed into a fine powder. Next, a [1 g of ZOE powder was weighting and added to aErlenmeyer flask 250 ml containing a 100 ml deionized water to dissolve. The mixture of conical was stirred and boiled at 70 °C for 30 min to form a colloidal yellow solution. The colloidal solution was treated by double filtration to remove the tiny solid pieces, resulting in a clear yellow solution. The final filtrate ZOE (1g/100 ml) solution was stored in a refrigerator-2 C for usein the next steps [7]. The complete characterizations (quantitative, qualitative, and spectroscopy diagnosis) for ZOE have been presented in the report of Abdulkadir Mohammed and his group [8].

Synthesis of copper nanoparticles [ZOE-CuNPs]

The process of bio-designing of ginger extract-based copper nanoparticles was performed in a ratio of 1:1 ml using as-prepared ZOE and copper acetate solutions. The process was conducted through mixing 25 ml of ZOE measured by a cylinder with 25 ml of copper acetate solution in a separate beaker [100 ml]. After that, the fluid in the beaker was agitated for an hour at room temperature. After the time stirring of the reaction mixture was ended, a colloidal greenish solution was formed, indicating on ZOE-CuNPs. Formation of greenish color is an assured phenomenon on the fabrication of CuNPs, which is confirmed and supported by many published reports (fig. 1). The final greenish result was then separated into two forms (liquid and solid) by centrifuging it for 15 min at 10,000 rpm. After removing the liquid phase, the solid nanoparticle phase was cleaned with distilled water and allowed to dry for a day. Next, the dry powder was collected in next day [9].

Fig. 1: Formation processes of ZOE-CuNPs

ZOE-CuNPs characterization

UV-Visible Spectroscopy: The development of CuNPs was recognized by recording the UV-Visible interest spectrum on a UV-i1900 double-beam spectrophotometer in the range of 250–700 nm. Dynamic Light Scattering (DLS) was utilized to measure the median size of particles and surface electrical charge (zeta potential) for the produced ZOE-CuNPs at room temperature using a Malvern Zetasizer-Nano device (Malvern, UK). X-Ray Diffraction (XRD): An X-ray diffractometer was used to examine the average size before crystallinity of CuNPs. The Debye-Scherrer formula was used to determine the crystallite size. Energy-dispersive X-ray spectroscopy (EDS) and scanning electron microscopy (SEM) were utilized to determine the elemental composition and confirm the existence of carbon, oxygen, and copper, SEM was also used to visualize the shape of nanoparticle. Fourier-Transform Infrared Spectroscopy (FT-IR): To regulate which functional groups are accountable for the stability and reduction of CuNPs, FT-IR spectroscopy was employed (Shimadzu IRAffinity-1S). Spectra were recorded between 4000–400 cm^{-1}.

Cytotoxicity evaluation against breast cancer cells

The analysis MTT was utilized to evaluate the synthesized ZOE-CuNPs' cytotoxicity towards human breast cancer cells, specifically AMJ13. The cells were permitted to adhere overnight after being plated at a density of 1×10^4 cells/well in 96-well plates. After that, they received 72 h of treatment with varying amounts of ZOE-CuNPs (0–100 µM). Following incubation, each well received 28 µl of MTT solution (2 mmol), which was then incubated for two hours at 37 °C. After removing the supernatant, formazan crystals were allowed to dissolve in DMSO. After a gentle shake, the plates were incubated at 37 °C for 15 min [10]. A microplate reader was utilized to determine the absorbance at 570 nm. The formula below is used to determine cell viability [1 and 2]:

$$\text{Proliferation rate (PR\%)} = \left(\frac{\text{OD treated}}{\text{OD control}}\right) \times 100 \ldots\ldots\ldots\ldots\ldots\ldots\ldots\ldots (1)$$

$$\text{Inhibition rate (IR\%)} = 100 - \text{PR\%} \ldots\ldots\ldots\ldots\ldots\ldots\ldots\ldots\ldots\ldots\ldots\ldots\ldots (2)$$

Statistical analysis

Normality has been determined using the Shapiro-Wilk and homogeneity of variances on the basis of the Levene test. ANOVA with Tukey HSD test was used when hypotheses were supported, otherwise the Kruskal-Wallis HSD test with Dunn-Bonferroni corrections were done. The data analysis was conducted through means comparison (with standard errors [or median quartile range]) when they were normally distributed. Report effect sizes (#2226 medicoadjkv GENETЩbell Arch naturally| consequently (eta square, ANOVA; r/ep squares, non-parametric tests) and exact statistics risky decimals 95 percent confidence interval of the pairwise comparison). The design was that of six dose groups (k=6) and three replicates in each dose group (n=3; total N=18). Analyses were carried out in GraphPad Prism 9.5.1 at alpha = 0.05.

RESULTS AND DISCUSSION

Confirmation of ZOE-CuNPsnanosize formation

ZE extract was used in this investigation to create ZOE-CuNPs by mixing and stirring. A UV-visible spectrophotometer was utilized to characterize produced ZOE-CuNPs. The lowering of copper ions

was verified by a color shift that was seen during precursor reduction. The UV-visible absorption spectra in the 250–700 nm range are shown in fig. 2 as the precursor matured and changed into ZOE-CuNPs under typical circumstances. Copper oxidation from a zero to an II oxidation state was shown by the ZOE-CuNPs' high absorption peak at 439 nm, which progressively darkened to a brown hue. The tight size distribution that occurs the particles is indicated by the strong peak at 439 nm. The solution's absorption spectra held steady even after a month of aging [11]. This colloidal brown solution has subjected to DLS and Zeta potential analysis, to confirm the obtained solution stability. The recorded results showed excellent values as explained in the fig.1b and c, indication on well preparation and stability of ZEO-CuNPs during different times.

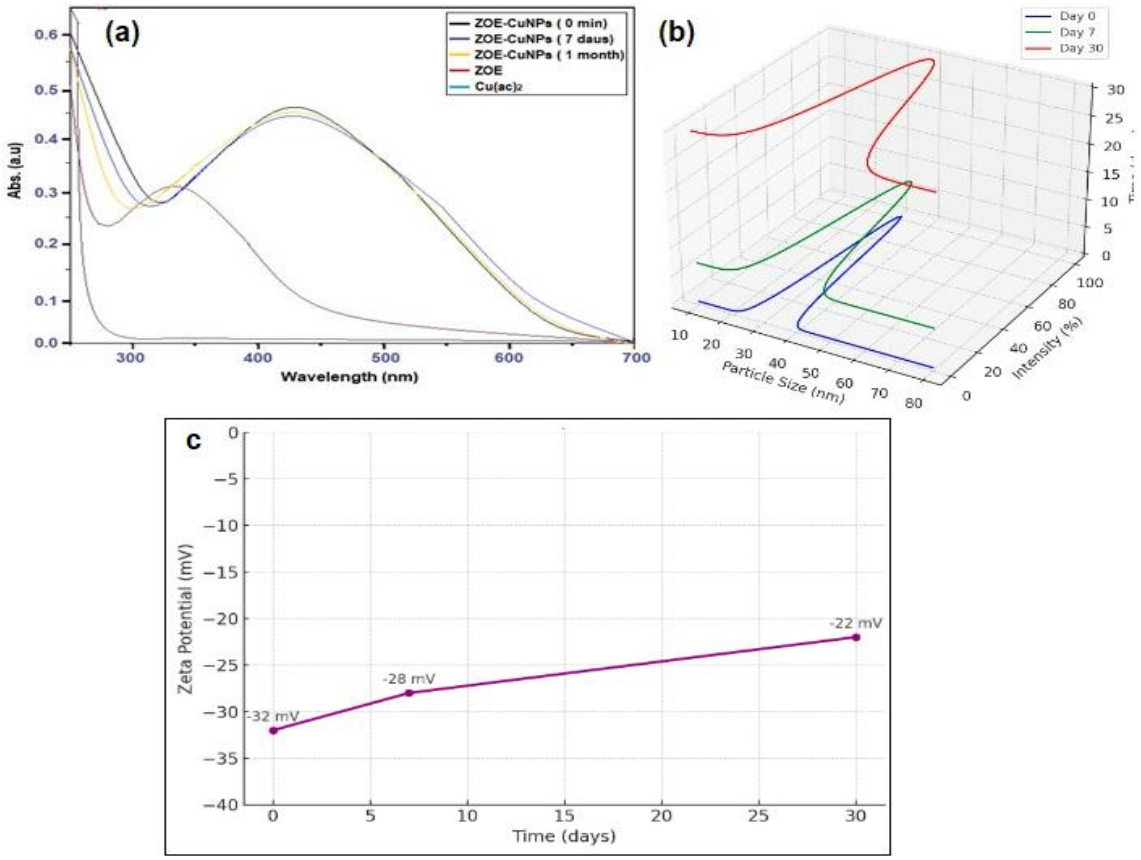

Fig. 2: a) UV-Vis analysis and b) DLS diagnosis and c) Z. potential test of ZOE-CuNPs during different times

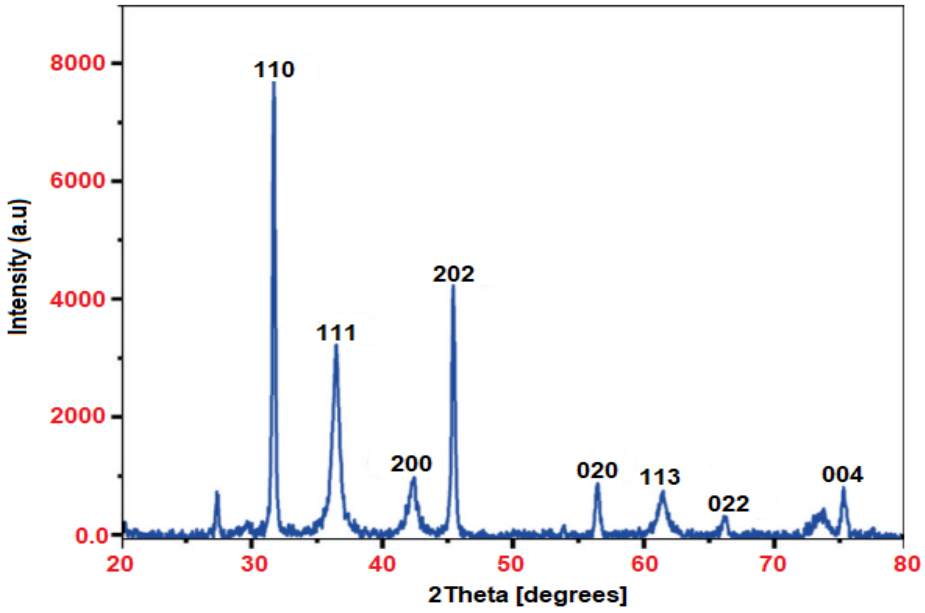

Fig. 3: XRD characterization of ZOE-CuNPs

XRD analysis of ZOE-CuNPs

The crystalline structure of ZOE-CuNPs was investigated using XRD techniques. The XRD spectrum (fig. 3) revealed peaks corresponding to the following crystallographic planes: (110) at 33.06°, (111) at 37.15°, (200) at 42.50°, (202) at 45.07°, (020) at 56.70°, (113) at 61.95°, (022) at 65.05°, and (044) at 76.52°. The recorded values return to (110), (111), (200), (202), (020), (113), (022), and (044). The XRD pattern of ZOE-CuNPs displayed a prominent peak at 33.06°, representing dominant growth along the (110) plane. All diffraction peaks for CuNPs confirm their crystallization in a face-centered cubic (FCC) structure (JCPDS 80–1268). Using the *Debye–Scherrer* equation, the calculated average particle size of ZOE-CuNPs was approximately 31 nm [12].

Morphology formation of ZOE-CuNPs

The structure and morphology of ZOE-CuNPs were stayed investigated. Measured and evaluated using scanning electron microscopy (SEM). The particles exhibited little clumping and were primarily quasi-spherical in shape, with a few irregular shapes discernible in the SEM images (fig. 4a). Using SEM imaging, monodispersed ZOE-CuNPs were seen on the ZOE matrix surface. Furthermore, fig. 4b illustrates how energy-dispersive X-ray analysis (EDS) is used to detect ZOE-CuNPs. Through noticeable peaks in the EDS spectrum, the composition of elements analysis verified the existence of carbon (C), copper (Cu), and oxygen (O). The emergence of a copper peak in the EDS spectrum further confirmed the presence of ZOE-CuNPs [13].

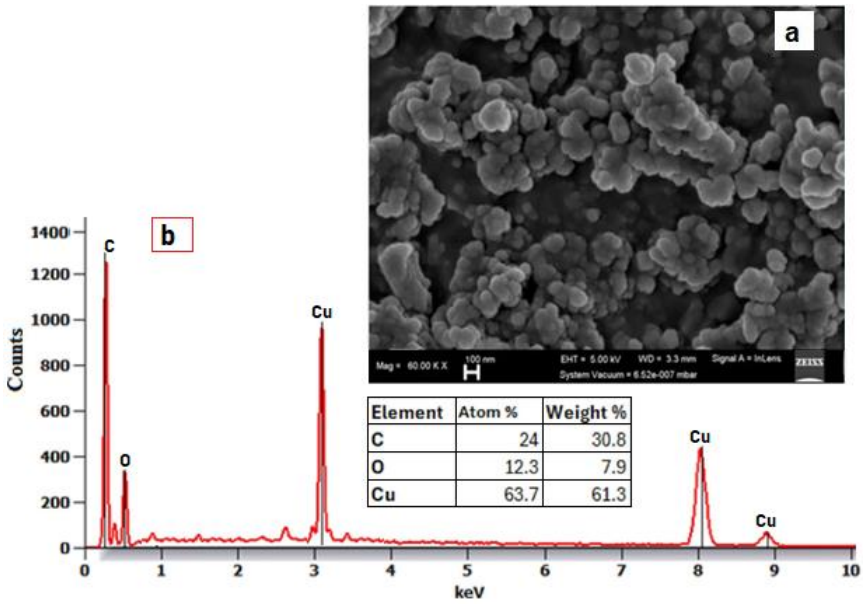

Fig. 4: a) SEM and b) EDS analysis of obtained ZOE-CuNFT-IR analysis of ZOE-CuNPs

The groups functionally involved in the reduction and stabilization of ZOE-CuNPs utilizing the ZOA extract were identified with the use of FTIR spectrum analysis. Distinct peaks at 1004, 1479, 1655, 2001, 2352, and 3352 1/cm were found when the FTIR spectra (fig. 5) of the ZO extract and the ZE extract-stabilized CuNPs were compared. These peaks corresponded to the C–O–C stretching, N–H stretching, C=C stretching, and CO2 stretching vibrations, respectively. However, C–O–C stretching, C–O stretching, –CH bending scissoring, C=C stretching, C–H stretching of alkanes, acute C–H stretching, and O–H stretching vibrations were responsible for the peaks that the synthesized CuO NPs displayed at 1022, 1249, 1430, 1522, 1749, 2906, 3252, and 3537 cm, individually. The observed spectral shifts in the ranges of 3248–3355 1/cm, 1652–1751 1/cm, and 1479–1432 1/cm indicate the possible presence of alcohol, carbonyl, and amine groups. These shifts indicate that the gingerol compound in ZEO extract components promoted the reduction of Cu^{2}+ions and the stabilization of ZEO-CuNPs. The production and growth of ZOE-CuNPs, which were too similar to the ZOE-AgNPs report, were significantly influenced by these functional groups in the ZO biocomponents [14, 15].

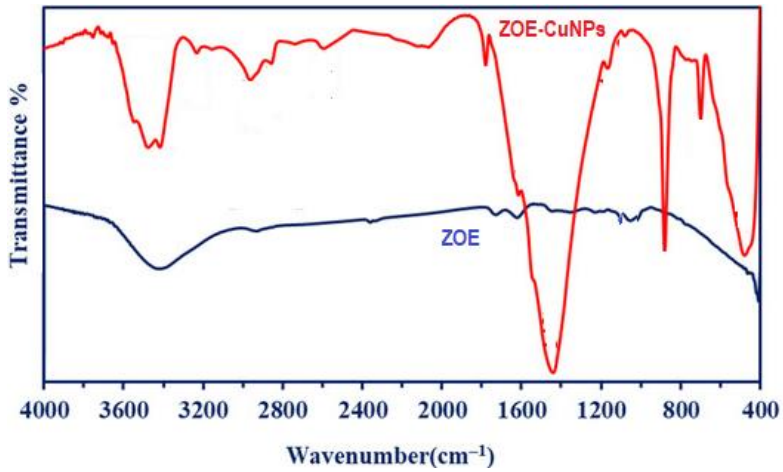

Fig. 5: FTIR analysis of ZOE and ZOE-CuNPs

Cytotoxicity evaluation against breast cancer cells

Table 1 indicates the inhibitory effect of various concentrations of ZOE-CuNPs on the breast cancer cells, as estimated using the MTT assay. There was a clear dose-response increase in Inhibition Rate (IR%) as the concentration of ZOE-CuNPs was increased from 0 to 100 µM. At 0 µM (control), the IR% was 0.00±2.1%, indicating no cytotoxicity. At 10 µM, inhibition began to appear (18.75±2.3%) and continued to rise progressively to 75.00±2.9% at 100 µM [16].

CuNPs reduced AMJ13 viability in a dose-dependent manner across the range of concentrations of 6 (0-100 mm; n = 3/group). The compilation effect of dose on inhibition rate was high (one-way ANOVA, F(5,12) = 124.56, p = 6.53 x 10-10, eta 2 = 0.981). The HSD test of Tukey divided each dose into different clusters of letters (a-f). Specifically, the mean difference between 100 uM and the largest (75.00 percentage points; 95% CI 66.88 to 83.12; p<0.001) was the control. Value of mean\(\pm\) SE and letter annotation are presented in table 1 and fig. 6.

Table 1: Cytotoxic impact of ZOE-CuNPs on breast cancer cells (MTT assay)

ZOE-CuNPs concentration (µM)	Inhibition rate (IR%) ±standard error (SE)
0	0.00±2.1a
10	18.75±2.3b
25	37.50±2.6c
50	56.25±2.8d
75	68.75±3.0e
100	75.00±2.9f
p-value	0.000***

Significance letters were assigned based on the Tukey HSD post hoc test (p<0.05). Groups sharing different letters are significantly the different data are mean±SE, n = 3/subgroup. One-way ANOVA F(5,12)=124.56, p=6.53×10^{-10}; Tukey's HSD: groups differ at p<0.05 when their labels do not share a letter.

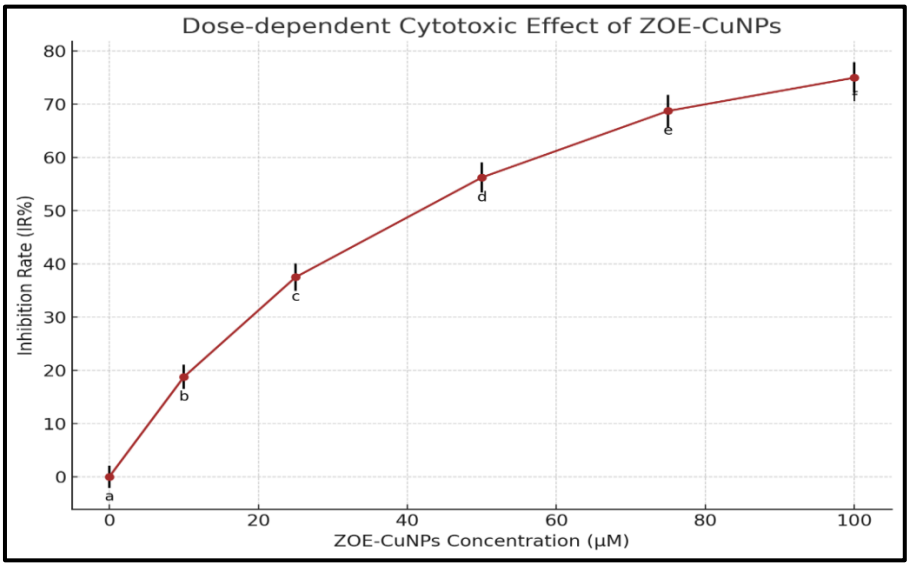

Fig. 6: Cytotoxicity evaluation of ZOE-CuNPs against breast cancer cells

The results of the current work demonstrate a concentration-dependent cytotoxic effect of phytochemically synthesized copper nanoparticles of *Zingiberofficinale* (ZOE-CuNPs) on breast cancer cells. The trend follows postulation that, due to nano-size, reactivity at the surface, and functionalization by bioactive constituents of the plant, phytochemically produced copper nanoparticles have enhanced biological activity.

The cytotoxicity manifested can be explained by the following mechanisms:

Copper ions have been shown to generate reactive oxygen species (ROS) in the cellular microenvironment, leading to oxidative stress, mitochondrial injury, and ultimately apoptotic cell death.

Adsorption of ginger-derived phytochemicals (e. g., gingerol, shogaol) onto the particle surface may enable cellular uptake and synergistically engage in pro-apoptotic activity through modulation of key cancer survival pathways such as PI3K/Akt/mTOR and NF-κB.

The progressive increase in inhibition rates again validates the suggested dose optimization strategy for ensuring maximum therapeutic effect with minimal systemic toxicity.

Statistically significant differences at all investigated concentrations emphasize the high therapeutic activity of ZOE-CuNPs in anticancer nanomedicine. Outcomes are consistent with current literature, testifying to green-synthesized metal nanoparticles being employed for anticancer-targeted application due to biocompatibility, eco-friendliness, and enhanced functional ability [17].

CONCLUSION

The present study confirms the effective synthesis of copper nanoparticles copper nanoparticle nanopark nanoparticle by*Zingiber* officinale extract (ZOE-CuNPs) and reports their significant cytotoxicity against breast cancer cells. Detailed physicochemical characterization revealed uniform, quasi-spherical particles with increased crystallinity and stability. Cytotoxicity assay revealed a clear dose-dependent inhibition of growth of cancer cells with statistical differences at all concentrations tested. The findings validate the potential of ZOE-CuNPs as a viable nanotherapeutic agent for targeted cancer therapy, which is worth further in vivo and clinical investigation.

ACKNOWLEDGMENT

Our research group acknowledges Nineveh University and the College of Pharmacy for assistance, guidance, and support.

FUNDING

Nil

AUTHORS CONTRIBUTIONS

Aymn Yaseen Sharaf Zeebaree: Conceptualization, Writing-original draft. Najat Ameen Saeed; Conceptualization, Writing-original draft. Abeer Mansour Abdel Rasool; Conceptualization, Writing, Review, and editing.

CONFLICT OF INTERESTS

Declared none

REFERENCES

1. Begum SA, Rani S J, Banu A, Pavani A, Yeruva V. Statistics of cancer, 2020 in Indian states: a review on the report from national cancer registry programme. Asian J Pharm Clin Res. 2021;14(6):36-42. doi: 10.22159/ajpcr.2021.v14i6.41616.
2. Kurul F, Turkmen H, Cetin AE, Topkaya SN. Nanomedicine: how nanomaterials are transforming drug delivery, bio-imaging and diagnosis. Next Nanotechnol. 2025;7:100129. doi: 10.1016/j.nxnano.2024.100129.
3. Sukandar EY, Kurniati NF, Wikaningtyas P, Agprikani D. Antibacterial interaction of combination of ethanolic extract of Zingiber officinale var rubrum rhizome, Boesenbergia pandurata rhizome, and Stevia rebaudiana leaves with certain antibiotics against infectious mouth microbial. Asian J Pharm Clin Res. 2016;9(1):332-5.
4. Jeena K, Liju VB, Kuttan R. Antioxidant, anti-inflammatory and antinociceptive activities of essential oil from ginger. Indian J Physiol Pharmacol. 2013;57(1):51-62. PMID 24020099.
5. Saeed Z. Garlic and ginger extracts mediated green synthesis of silver and gold nanoparticles: a review on recent advancements and prospective applications. Biocatal Agric Biotechnol. 2023 Oct;53:102868. doi: 10.3126/jncs.v39i0.27008.
6. Oli HB, Sharma N, KC E, Subedee A, Timilsina R. Green synthesis of copper nanoparticles using Zingiber officinale extract and characterization. J Nepal Chem Soc. 2020;39:10-7. doi: 10.3126/jncs.v39i0.27008.
7. Alkhyatt MM, Rasool AM, Daood GS. Detoxification of hydrocyanide by fermentation of apricot seeds with probiotic Lactobacillus strains isolated from breast milk. Regul Mech Biosyst. 2025;15(4):661-5. doi: 10.15421/022495.
8. Chandrappa CP, Chandrasekar N, Govindappa M, Shanbhag C, Singh UK, Masarghal J. Antibacterial activity of synthesized silver nanoparticles by Simarouba glauca against pathogenic bacteria. Int J Curr Pharm Sci. 2017;9(4):19-22. doi: 10.22159/ijcpr.2017v9i4.20629.
9. Ismail Haji Zebari O, Yaseen Sharaf Zeebaree S, Yaseen Sharaf Zeebaree A, Ismail Haji Zebari H, Ridha Abbas H. Antibacterial activity of copper nanoparticles fabricate via malva sylvesteris leaf extract. Kurdistan J Appl Res. 2019;4(3):146-56. doi: 10.24017/science.2019.ICHMS.15.
10. Ahmed MF, A. Design synthesis of novel quinazolin-4-one derivatives and biological evaluation against human MCF-7 breast cancer cell line. Res Chem Intermed. 2016;42(3):1777-89. doi: 10.1007/s11164-015-2117-z.
11. Amaliyah S, Pangesti DP, Masruri M, Sabarudin A, Sumitro SB. Green synthesis and characterization of copper nanoparticles using Piper retrofractum Vahl extract as bioreductor and capping agent. Heliyon. 2020;6(8):e04636. doi: 10.1016/j.heliyon.2020.e04636, PMID 32793839.
12. Bragg WH. The analysis of crystal structure by x-rays. Science. 1924;60(1546):139-49. doi: 10.1126/science.60.1546.139, PMID 17750761.
13. Al Jubouri AK, Al Saadi NH, Kadhim MA. Green synthesis of copper nanoparticles from Myrtus communis leaves extract: characterization, antioxidant and catalytic activity. Iraqi J Agric Sci. 2022;53(2):471-86. doi: 10.36103/ijas.v53i2.1555.
14. Liu X. IR spectrum and characteristic absorption bands. J Org Chem. 2021;I. doi: 10.1016/j.ceramint.2021.08.268.
15. He X, Liu X, Nie B, Song D. FTIR and Raman spectroscopy characterization of functional groups in various rank coals. Fuel. 2017;206:555-63. doi: 10.1016/j.fuel.2017.05.101.
16. Ulukaya E, Ozdikicioglu F, Oral AY, Demirci M. The MTT assay yields a relatively lower result of growth inhibition than the ATP assay, depending on the chemotherapeutic drugs tested. Toxicol *In Vitro*. 2008;22(1):232-9. doi: 10.1016/j.tiv.2007.08.006, PMID 17904330.
17. Brahmbhatt M, Gundala SR, Asif G, Shamsi SA, Aneja R. Ginger phytochemicals exhibit synergy to inhibit prostate cancer cell proliferation. Nutr Cancer. 2013;65(2):263-72. doi: 10.1080/01635581.2013.749925, PMID 23441614.